A Coordinated Planning and Operational Optimization Framework for Agrivoltaic Microgrids

Guanning Li, Richard Mahuze, Qirui Long and K. Max Zhang
Sibley School of Mechanical and Aerospace Engineering
Cornell University
Ithaca, NY, USA, 14853
gl548@cornell.edu, ram552@cornell.edu, ql346@cornell.edu, and kz33@cornell.edu

***Abstract*—This paper proposes a coordinated planning and operational optimization framework for grid-connected agrivoltaic microgrids. The framework integrates interdependent optimization modules to address long-term capacity planning and short-term operational control under agrivoltaic constraints. Planning decisions determine photovoltaic and battery capacities, while operational optimization governs solar panel tilt and battery charging and discharging under time-of-use tariffs. A virtual case study using open-source datasets demonstrates the applicability of the proposed framework. The resulting optimal planning capacities are compared with those from other solar farm designs, highlighting the importance of accounting for operational constraints in agrivoltaic microgrid planning.**

***Index Terms*—coordinated optimization framework, agrivoltaic microgrids, planning and operation**

I. Introduction

Sustainable energy transitions have gained increasing global attention. The Long-Term Strategy of the United States explicitly targets net-zero greenhouse gas emissions by 2050 [1]. In Europe, the European Green Deal and the European Climate Law commit the EU to becoming climate-neutral by 2050 and to reducing net greenhouse gas emissions by at least 55% by 2030 [2]. Rural areas play a pivotal role in achieving a renewable energy future. In the United States, rural regions have a disproportionately large impact on national greenhouse gas emissions. Accounting for only 18% of the population, U.S. rural areas contribute more than 36% of total emissions. Moreover, more than 47% of all power plant emissions occur in rural areas [3]. Renewable resources such as solar and wind offer viable pathways to improve sustainability in these areas. However, their high land requirements conflict with existing agricultural and ecological uses, leaving limited land available for renewable energy deployment without disrupting current functions [4].

Agrivoltaics (APV) is a dual-land-use strategy that integrates agricultural production with solar energy generation on the same land parcel, offering a promising solution to land–energy conflicts. The feasibility has been well examined [5]. By enabling synergistic rather than competitive outcomes, APV can relieve pressure on agricultural land, enhance solar efficiency through microclimatic effects, improve yields for certain crops, and increase overall economic returns via combined energy and agricultural production [6]. Additionally, solar-tracking strategies in APV systems have been widely studied to further enhance their attractiveness. Existing APV tracking studies mainly investigate how panel orientation and motion regulate light sharing between crops and photovoltaic (PV) modules. Prior work considers standard single-axis tracking, adaptive or crop-oriented strategies, and, in some cases, combinations of standard and reverse tracking, with performance evaluated using metrics such as photosynthetically active radiation (PAR), crop yield, or solar energy output under specific operational conditions [7]–[9].

These advantages make APV particularly attractive in rural regions, where energy delivery costs are higher due to low population densities and dispersed loads [10]. In such contexts, renewable-based microgrid systems can further improve reliability, resilience, and economic performance by providing localized generation and storage, reducing dependence on long transmission lines, and enhancing operational flexibility [11]. Together, APV and microgrids present a complementary solution for sustainable rural energy development.

However, most existing APV and distributed energy system studies, including those on PV and wind turbine (WT) systems, focus on component-level sizing or high-level optimization, leaving an important gap [12]–[14]. While microgrid energy management strategies are well studied, their integration within APV systems remains limited [15]. In particular, agrivoltaic-specific operational decisions, such as solar tracking strategies, can significantly affect solar output and, consequently, optimal system sizing, yet are rarely incorporated into long-term planning frameworks.

To address this gap, this paper develops a coordinated optimization framework for agrivoltaic microgrids integrating PV systems under agrivoltaic constraints, battery energy storage, and grid interaction. The coordinated treatment of short-term operational control and long-term capacity planning within a hierarchical formulation is realized. By explicitly linking hourly operational decisions, including solar tracking, with multi-year system sizing, the proposed framework identifies PV and battery configurations that better reflect the operational characteristics of agrivoltaic microgrids.

II. Optimization Framework Description

A. Framework Flowchart Overview

The proposed framework integrates long-term planning optimization and short-term operational optimization to achieve

979-8-3315-8138-1

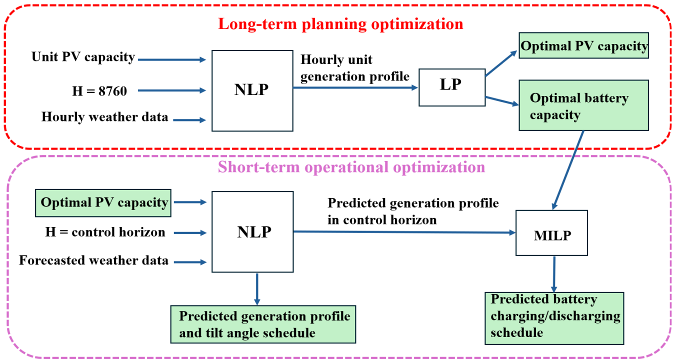

Fig. 1: Workflow of the proposed framework

both economic and operational efficiency in an APV microgrid. The overall workflow is illustrated in Fig. 1. Green blocks highlight critical outputs from planning and operational optimization.

A nonlinear programming (NLP) model is used to capture the nonlinear relationships among shadow width, solar generation calculations, and other agrivoltaic variables. A linear programming (LP) model is adopted for capacity planning due to its simplicity and tractability, while a mixed-integer linear program (MILP) is used to explicitly model battery charge and discharge behavior, rather than relying on a single scalar state-of-energy representation.

In the long-term planning optimization, hourly weather data for an entire year are first input into the NLP model. The NLP model estimates the hourly solar generation profile, subject to specific constraints in the agrivoltaic context, for a unit with full-year capacity, producing a unit generation profile. This normalized generation profile is then passed to the LP model, which determines the optimal PV and battery capacities that minimize system costs.

In the short-term operational optimization, the PV capacity determined in the planning stage is provided to the NLP model. The NLP model uses forecasted weather data over an optimization horizon to maximize solar production subject to operational constraints. The resulting generation profile, together with forecasted load, is then passed to the MILP model, which computes the optimal battery charging and discharging schedule that minimizes power import costs over the same horizon. As forecasts update, the optimization is recalculated at each step, enabling adaptive, data-driven operational decisions. In realistic applications, optimization-based control or other control schemes can ensure consistency throughout the lifetime of microgrid operation [16].

The integration of long-term and short-term optimization enables coordinated decision-making, with strategic capacity planning and hourly operational actions informing one another. Each optimization component is described in detail in the following subsections.

B. LP Model for Solar & Battery Capacity Planning

The renewable power system optimization problem is formulated as an LP that minimizes the total system cost while satisfying energy balance and technical constraints at each hourly time step $t \in \mathcal{T} = \{0, 1, \ldots, T-1\}$.

1) Decision Variables: Components of variables set $\mathbb{V}_1$ are:

S_{PV} : installed PV capacity(kW_{AC})

C_{bat} : installed battery capacity (kWh)

SOE_t : battery state of energy (kWh)

$P_t^{x \to y}$: hourly power flow from x to y (kW)

x and y represent two of the microgrid components including PV, battery and utility.

Every variable in $\mathbb{V}_1$ is assumed nonnegative.

2) Constraints:

Power Balance: The available solar generation at each time step is given by

$$G_t^{\text{PV}} = P_t^{\text{u}} \cdot S_{\text{PV}} \tag{1}$$

where P_t^{u} is the unit solar generation at time t.

The renewable electricity distributed from the PV system to the load and to the battery must not exceed the total available generation:

$$P_t^{\text{PV}\to\text{load}} + P_t^{\text{PV}\to\text{bat}} \leq G_t^{\text{PV}} \tag{2}$$

The electricity demand of the household must be met by the combined supply from solar generation, battery discharge, and utility power:

$$P_t^{\text{PV}\to\text{load}} + P_t^{\text{bat}\to\text{load}} + P_t^{\text{util}\to\text{load}} = D_t \tag{3}$$

where D_t denotes the hourly electricity demand.

Battery Dynamics: The SOC (state of charge) of the battery must remain within allowable limits, leading to the following inequality involving SOE_t as variables:

$$C_{\text{bat}} \cdot \text{SOC}_{\text{min}} \leq \text{SOE}_t \leq C_{\text{bat}} \tag{4}$$

where SOC_{min} represents the minimum allowable SOC.

The SOE evolves according to

$$\text{SOE}_t = \begin{cases} \text{SOE}_0 = \text{SOC}^{\text{init}} \cdot C_{\text{bat}}, & t = 0 \\ \text{SOE}_{t-1} + (P_t^{\text{PV}\to\text{bat}} + P_t^{\text{util}\to\text{bat}}) \cdot \eta_{\text{ch}} & \\ -P_t^{\text{bat}\to\text{load}} / \eta_{\text{dis}} & t > 0 \end{cases} \tag{5}$$

where SOC^{init} is the initial battery state of charge, η_{ch} and η_{dis} the battery charging and discharging efficiency. Note that with a one-hour time resolution, power in kW is numerically equal to energy in kWh.

Battery charging and discharging rates are limited by the maximum power rate of the battery:

$$P_t^{\text{bat}\to\text{load}} \leq C_{\text{bat}} \cdot r_{\text{max}} \tag{6}$$

$$P_t^{\text{PV}\to\text{bat}} + P_t^{\text{util}\to\text{bat}} \leq C_{\text{bat}} \cdot r_{\text{max}} \tag{7}$$

where r_{max} is the battery's maximum charging/discharging rate in percentage.

979-8-3315-8138-1

3) Objective Function: The optimization objective is to minimize the system's equivalent annual cost (EAC), including investment, operation, and maintenance (O&M), and utility electricity costs.

$$\min_{\mathbb{V}_1} \text{ EAC} = C_{\text{PV,annual}} + C_{\text{bat,annual}} + C_{\text{upp}} \tag{8}$$

Each term in (8) is detailed as follows:

Annual Cost of PV and Battery Systems: For each asset $x \in \{\text{PV}, \text{bat}\}$, the equivalent annual cost is

$$C_{x,\text{annual}} = I_x \cdot \text{CRF}_N + I_x \cdot \gamma_{x,\text{O\&M}} \tag{9}$$

where I_x is the upfront investment, $\gamma_{x,\text{O\&M}}$ the O&M cost rate and CRF_N the capital recovery factor for a lifetime of N years.

Annual Utility Power Purchase Cost: The annual operating cost for grid electricity purchases is given by

$$C_{\text{upp}} = \sum_{t \in \mathcal{T}} \left(P_t^{\text{util}\rightarrow\text{load}} + P_t^{\text{util}\rightarrow\text{bat}} \right) \cdot \left(p_{\text{del}} + p_{\text{sup},t} \right) \cdot (1+\alpha) \tag{10}$$

where p_{del} is the utility power delivery charge, $p_{\text{sup},t}$ the utility power supply price, based on time-of-use tariff rate and α accounts for applicable surcharges or taxes rate.

C. NLP Model for Solar Panel Tilt Angle Control

The NLP model determines the optimal panel tilt angle trajectory, θ_t, over a certain simulation horizon, $t \in \mathcal{H}_s = \{0, 1, \ldots, H_s - 1\}$, to maximize total energy production while maintaining acceptable shading, backtracking, and plant growth conditions. This formulation preserves robustness and tractability while allowing economic and agronomic factors to be incorporated in specific engineering contexts.

Decision Variable:

$$\theta_t \in [-\theta_{\max}, \theta_{\max}], \quad \forall t \in \mathcal{H}_s \tag{11}$$

where $\theta_{\max}$ is the maximum tolerable tilt angle.

Constraints:

a) Shadow Width: The shadow cast by one row should not fall on the panels of the neighboring rows. Therefore, the shadow width (w_t^{shad}) is constrained by:

$$0 \leq w_t^{\text{shad}} \leq S_p \tag{12}$$

and the formula for calculating w_t^{shad} is:

$$w_t^{\text{shad}} = \left(\frac{\sin \phi_r(t)}{\tan \theta_e(t)} \sin \theta_t + \cos \theta_t \right) \cdot w_p \tag{13}$$

where w_p is the panel width, S_p the pitch distance, ϕ_r the relative solar azimuth angle (difference between solar azimuth and solar panel rows azimuth) and θ_e the solar elevation angle.

b) Crop Growth Requirement: The Daily Light Integral (DLI) quantifies the accumulated PAR received by the crop canopy over 24 hours and is widely used as a species-independent indicator of daily light availability for photosynthesis and biomass production. In practice, policy and subsidy requirements may also mandate minimum crop production levels, which can be enforced by specifying appropriate DLI targets or constraints [17].

Therefore, a constraint on DLI, defined as (14), ensures the crop can grow normally in an agrivoltaic context.

$$\frac{1}{H_s} \sum_{t \in \mathcal{H}_s} \text{DLI}_t \geq \text{DLI}_{\text{target}} \tag{14}$$

In this framework, DLI is calculated based on ground radiation, considering both direct normal irradiance (DNI) and diffuse horizontal irradiance (DHI), expressed by

$$I_t^{\text{gnd}} = \left(1 - \frac{w_t^{\text{shad}}}{S_p} \right) \sin(\theta_e(t)) \cdot \text{DNI}_t + f_t^{\text{diff}} \cdot \text{DHI}_t \tag{15}$$

where f_t^{diff}, diffuse fraction, is a polynomial of θ_t calculated based on diffuse radiation integration between panel rows, accounting for sky obstruction using a discretized sky dome [18].

Finally, DLI (in $mol \cdot m^{-2} \cdot day^{-1}$) is calculated by

$$\text{DLI}_t = I_t^{\text{gnd}} \cdot f_{PAR} \cdot \epsilon_{PAR} \cdot 24 \cdot 3600/10^6 \tag{16}$$

where f_{PAR} is fraction of total solar irradiance that is PAR (dimensionless) and ϵ_{PAR} is quantum conversion coefficient (in $\mu mol/J$).

Objective Function: The objective of the NLP is defined as

$$\max_{\{\theta_t\}} \sum_{t \in \mathcal{H}_s} P_t \cdot p_{\text{sup},t} \tag{17}$$

where P_t denotes the PV power output at time t. The coefficient, $p_{\text{sup},t}$, denotes the time-of-use tariff rate. As typical TOU tariffs are uniform during most daylight hours when solar generation occurs, incorporating this coefficient into the objective function provides only a limited additional benefit and can be omitted for simplicity.

In the bifacial scenario, generation is determined by both front and back surface irradiance, denoted as I_t^{front} and I_t^{back}, respectively:

$$I_t^{\text{front}} = \cos(\text{AOI}_t)\, \text{DNI}_t + \text{DHI}_t\, f_t^+ + \alpha\, I_t^{\text{gnd}}\, f_t^- \tag{18}$$

$$I_t^{\text{back}} = \text{DHI}_t\, f_t^- + \alpha\, I_t^{\text{gnd}}\, f_t^+ \tag{19}$$

where AOI represents the angle of incident (angle between sunlight and normal of any solar panel), α represents surface albedo, and f_t^+ and f_t^- represent the sky view factors for the front and back surfaces, respectively.

Solar generation of solar panels can be expressed by

$$P_t = P_{\text{PV}}^{\text{rated}} \frac{I_t^{\text{front}} + \kappa I_t^{\text{back}}}{1000} \left[1 + \Gamma(T_t^{\text{cell}} - T_{\text{ref}}) \right] \tag{20}$$

where $P_{\text{PV}}^{\text{rated}}$ is the PV nameplate capacity, κ the bifaciality factor, Γ the temperature coefficient of the solar panels, T_t^{cell} the cell temperature at time t, and T_{ref} the reference temperature [19].

D. MILP Model for Battery Operation Management

The battery scheduling problem is formulated as an MILP model that optimizes the behavior of a battery energy storage system over a time horizon $\mathcal{H}_b = \{0, 1, \ldots, H_b - 1\}$, given a solar generation profile and a battery capacity. The optimization seeks to minimize the cost of electricity imported from the utility.

1) Decision Variables: Components of variables set $\mathbb{V}_2$ are:

$P_t^{\text{ch}}, P_t^{\text{dis}}$	: battery charging/discharging power (kW)
SOE_t	: battery state of energy (kWh)
m_t^{ch}, m_t^{dis}	: binary indicators for charging/discharging modes
$P_t^{x \to y}$	: power flow from component x to y (kW)

Every variable in $\mathbb{V}_2$ is assumed nonnegative.

2) Constraints:

Mutual Exclusivity of Charging and Discharging: The battery cannot charge and discharge simultaneously:

$$m_t^{\text{ch}} + m_t^{\text{dis}} \leq 1 \tag{21}$$

Power Balance and Battery Dynamics: The power balance, battery charging/discharging power constraints and SOE evolution rule are detailed in (3)–(7) and here are adopted again.

Battery Charging Source: In this model, battery charging power can be from solar generation and utility:

$$P_t^{\text{ch}} = P_t^{\text{PV}\to\text{bat}} + P_t^{\text{util}\to\text{bat}} \tag{22}$$

P_t^{dis} is not specified because it is essentially equivalent to $P^{\text{bat}\to\text{load}}$ (Feed-in to the utility is not considered).

3) Objective Function: The objective is to minimize the total utility grid import cost:

$$\min_{\mathbb{V}_2} \sum_{t\in\mathcal{H}_b} \left(P_t^{\text{util}\to\text{load}} + P_t^{\text{util}\to\text{bat}}\right) \cdot \left(p_{\text{del}} + p_{\text{sup},t}\right) \cdot (1+\alpha) \tag{23}$$

III. Case Study of the Agrivoltaic Microgrid Application

To demonstrate the applicability of the proposed framework, a virtual case study is conducted. Public data are collected and the framework is implemented. Both long-term planning and short-term operational problems are solved based on the scheme stated in Fig. 1.

A. Data Overview and Model Implementation

An open-source load profile for a dairy farm is adopted [20]. The dataset represents a farm with approximately 180 cows and an annual electricity consumption of around 275 MWh. The dataset is used hypothetically to represent an agrivoltaic farm scenario. Weather data is obtained from the US National Solar Radiation Database [21]. Attributes selected are DNI, DHI and temperature. Other weather data involved in calculation, including ϕ_r and θ_e, are retrieved using the pvlib library [22]. The calculation for the I_x, upfront investment of PV and battery are based on U.S. Solar Photovoltaic System and Energy Storage Cost Benchmarks, Q1, 2023 [23]. Other input parameters are detailed in Table I.

TABLE I: Model Parameters

Symbol	Description	Value	Unit
SOC^{init}	Battery initial state of charge	100	%
η_{ch}	Battery charging efficiency	95	%
η_{dis}	Battery discharging efficiency	95	%
SOC_{min}	Minimum tolerable SOC	20	%
r_{max}	Battery's maximum power rate	25	%
N	Asset lifetime	25	year
$\gamma_{\text{O\&M}}$	Annual O&M cost rate	2.5	%
p_{del}	Utility power delivery charge	0.075	$/kWh
α	Applicable surcharges or taxes rate	5	%
$\theta_{\max}$	Maximum tolerable tilt angle	60	degree
S_p	Pitch distance	6	meter
κ	Bifaciality factor	0.8	–
Γ	Temperature coefficient of the solar panels	-0.3	%/°C
T_{ref}	Reference temperature	25	°C

Hourly weather data are first provided to the NLP model, with the simulation horizon set to $H_s = 8760$ and the nominal panel power set to $P_{\text{PV}}^{\text{rated}} = 1$ kW. The resulting optimized hourly unit solar generation profile is then used as input to the long-term planning LP model, which determines the optimal PV capacity S_{PV}, battery capacity C_{bat}, and the associated annualized cost of electricity (ACE), defined as the ratio of the equivalent annual cost (EAC) to the annual electricity demand.

With the optimal PV capacity S_{PV} and battery capacity C_{bat} determined from the planning stage, a short-term operational analysis can be conducted within the framework to evaluate APV microgrid performance under realistic operating conditions. Forecasted weather data can be provided to the NLP-based controller to determine an optimal tilt-angle trajectory over a representative control horizon.

Unlike conventional STPV operation, the APV control scheme incorporates crop-related constraints that restrict tilt-angle selection and prevent continuous operation at orientations that solely maximize solar energy yield. As a result, the optimal tilt-angle trajectory reflects a trade-off between maximizing solar generation and maintaining sufficient light availability for crops.

The solar generation profile implied by the optimized tilt-angle trajectory is subsequently passed to the MILP-based energy management model, which determines the optimal battery charging and discharging schedules as well as power exchanges with the utility grid. This control framework enables consistent coordination between APV-specific solar operation and microgrid-level energy management, capturing the operational impacts of agrivoltaic constraints on both renewable generation and storage dispatch.

B. Planning Results Comparison and Discussions

The planning results under different operational assumptions are examined and results are summarized in Table II. The results indicate that the unconstrained STPV case achieves a lower ACE and larger optimal battery and effective solar generation levels (despite a smaller installed nameplate capacity). This outcome arises because removing

TABLE II: Comparison of Three Microgrid Plans

	S_{PV} (kW$_{\text{AC}}$)	C_{bat} (kWh)	ACE (\$/kWh)	DLI
APV	173.85	193.51	0.190	25.000
STPV	154.35	346.13	0.149	17.593
Baseline	154.35	346.13	0.197	25.000

agrivoltaic operational constraints allows substantially higher solar energy yield, thereby creating an unrealistically strong economic incentive for PV deployment in an APV context. Such solutions, however, are not physically or agronomically feasible, as excessive shading (around 30% DLI sacrificed) would limit light availability for the crop and hinder normal plant growth. These findings highlight that conventional STPV-based planning can significantly overestimate the economic performance of agrivoltaic systems, underscoring the necessity of a planning framework explicitly tailored to APV operational constraints.

To further illustrate the importance of accounting for APV-specific operational conditions during planning, the system sized under the STPV scenario is subsequently operated while enforcing APV constraints (Baseline). This experiment represents a realistic but flawed workflow: a microgrid is designed assuming standard PV operation but later deployed as an APV system, where crop-related constraints, particularly DLI requirements, must be satisfied in practice. As shown in Table II, enforcing APV constraints during operation results in a higher ACE than that obtained with the proposed framework. For an annual electricity demand of 275 MWh, this mismatch results in approximately \$1925 of additional annualized cost, demonstrating the economic penalty associated with neglecting APV operational considerations during the planning stage.

IV. Conclusion

This work demonstrates that combining long-term planning with short-term optimization-based control can provide a coherent pathway for designing and operating agrivoltaic microgrids. The proposed framework demonstrates the impact of incorporating agrivoltaic constraints into the planning optimization. The case study illustrates the value of such coordination, revealing opportunities to improve both economic performance and the feasibility of agrivoltaic microgrids. Continued development of this approach could support broader deployment of agrivoltaic microgrids and strengthen their role in sustainable rural energy systems, especially with more case-specific considerations.

References

[1] "THE LONG-TERM STRATEGY OF THE UNITED STATES Pathways to Net-Zero Greenhouse Gas Emissions by 2050," 2021. Available: https://bidenwhitehouse.archives.gov/wp-content/uploads/2021/10/US-Long-Term-Strategy.pdf.

[2] "The European Green Deal," European Commission, Jul. 14, 2021. https://commission.europa.eu/strategy-and-policy/priorities-2019-2024/european-green-deal_en?.

[3] "Report: The Overlooked Climate Impact of Rural America — Rural Climate Partnership," Ruralclimate.org, 2024. https://ruralclimate.org/rural-emissions-report-2024/.

[4] J. Guo, V. Fast, P. Teri, and K. Calvert, "Integrating Land-Use and Renewable Energy Planning Decisions: A Technical Mapping Guide for Local Government," ISPRS International Journal of Geo-Information, vol. 9, no. 5, p. 324, May 2020, doi: https://doi.org/10.3390/ijgi9050324.

[5] P. E. Campana et al., "Scientific frontiers of agrivoltaic cropping systems," Nat. Rev. Clean Technol., pp. 1–21, Nov. 2025, doi: 10.1038/s44359-025-00110-9.

[6] P. E. Campana, B. Stridh, S. Amaducci, and M. Colauzzi, "Optimisation of vertically mounted agrivoltaic systems," Journal of Cleaner Production, vol. 325, p. 129091, Nov. 2021, doi: https://doi.org/10.1016/j.jclepro.2021.129091.

[7] M. Bruno, L. J. Gfüllner, and M. F. Berwind, "Enhancing agrivoltaic synergies through optimized tracking strategies," JPE, vol. 15, no. 3, p. 032703, Jan. 2025, doi: 10.1117/1.JPE.15.032703.

[8] M. H. Riaz, H. Imran, H. Alam, M. A. Alam, and N. Z. Butt, "Crop-Specific Optimization of Bifacial PV Arrays for Agrivoltaic Food-Energy Production: The Light-Productivity-Factor Approach," in IEEE Journal of Photovoltaics, Mar. 2022, pp. 572–580. doi: 10.1109/JPHOTOV.2021.3136158.

[9] A. Stuhlmacher, J. Mathieu, and P. Seiler, "Optimizing Dual-Axis Solar Panel Operation in an Agrivoltaic System and Implications for Power Systems," in Hawaii International Conference on System Sciences 2024 (HICSS-57), Jan. 2024. [Online]. Available: https://aisel.aisnet.org/hicss-57/es/renewable_resources/4/.

[10] "One in three U.S. households faces a challenge in meeting energy needs - Today in Energy - U.S. Energy Information Administration (EIA)," www.eia.gov. https://www.eia.gov/todayinenergy/detail.php?id=37072.

[11] S. Abu-Elzait and R. Parkin, "Economic and Environmental Advantages of Renewable-based Microgrids over Conventional Microgrids," IEEE Xplore, Apr. 01, 2019. https://ieeexplore.ieee.org/document/8767146 (accessed Mar. 07, 2021).

[12] R. Khezri, A. Mahmoudi, and H. Aki, "Optimal planning of solar photovoltaic and battery storage systems for grid-connected residential sector: Review, challenges and new perspectives," Renewable and Sustainable Energy Reviews, vol. 153, p. 111763, Jan. 2022, doi: https://doi.org/10.1016/j.rser.2021.111763.

[13] R. Tarife, Y. Nakanishi, Y. Chen, Y. Zhou, N. Estoperez, and A. Tahud, "Optimization of Hybrid Renewable Energy Microgrid for Rural Agricultural Area in Southern Philippines," Energies, vol. 15, no. 6, p. 2251, Mar. 2022, doi: https://doi.org/10.3390/en15062251.

[14] V. Tomar and G. N. Tiwari, "Techno-economic evaluation of grid connected PV system for households with feed in tariff and time of day tariff regulation in New Delhi – A sustainable approach," Renewable and Sustainable Energy Reviews, vol. 70, pp. 822–835, Apr. 2017, doi: https://doi.org/10.1016/j.rser.2016.11.263.

[15] A. Esparza, M. Blondin, and J. P. F. Trovão, "A Review of Optimization Strategies for Energy Management in Microgrids," Energies, vol. 18, no. 13, p. 3245, Jun. 2025, doi: https://doi.org/10.3390/en18133245.

[16] A. Amadeh, Q. Long, H. J. Williams, and K. M. Zhang, "An integrated control framework for optimal sunlight sharing in agrivoltaic systems," unpublished manuscript, 2026.

[17] T. Kumdokrub and F. You, "A Techno-Economic-Ecological Systems Approach to Sustainable Agrivoltaics Development: Current Advancements, Key Challenges, and Future Directions," ACS Sustainable Chem. Eng., Nov. 2025, doi: 10.1021/acssuschemeng.5c04919.

[18] M. A. Mikofski, R. Darawali, M. Hamer, A. Neubert, and J. Newmiller, "Bifacial Performance Modeling in Large Arrays," in 2019 IEEE 46th Photovoltaic Specialists Conference (PVSC), Jun. 2019, pp. 1282–1287. doi: 10.1109/PVSC40753.2019.8980572.

[19] K. S. Anderson, C. W. Hansen, W. F. Holmgren, A. R. Jensen, M. A. Mikofski, and A. Driesse, "pvlib python: 2023 project update," Journal of Open Source Software, vol. 8, no. 92, p. 5994, Dec. 2023, doi: 10.21105/joss.05994.

[20] S. Uski and E. Rinne, "Data for a dairy farm microgrid solution". Zenodo, Jun. 21, 2018. doi: 10.5281/zenodo.1294967.

[21] NREL, "NSRDB," nsrdb.nrel.gov. https://nsrdb.nrel.gov/data-viewer.

[22] W. F. Holmgren, C. W. Hansen, and M. A. Mikofski, "pvlib python: a python package for modeling solar energy systems," Journal of Open Source Software, vol. 3, no. 29, p. 884, Sep. 2018, doi: https://doi.org/10.21105/joss.00884.

[23] V. Ramasamy et al., "U.S. Solar Photovoltaic System and Energy Storage Cost Benchmarks, With Minimum Sustainable Price Analysis: Q1 2023," 2023. Available: https://www.nrel.gov/docs/fy23osti/87303.pdf.

979-8-3315-8138-1